Publ. Astron. Soc. Japan, **41**, 841–851 (1989)

One-Armed Instabilities of Flat Stellar Disks with a Different Amount of Retrograde Stars

Shunsuke HOZUMI*

Department of Astronomy, Faculty of Science, University of Kyoto, Kitashirakawa, Sakyo-ku, Kyoto 606

and

Takao FUJIWARA

Kyoto City University of Arts, Oekutsukakecho, Nishikyo-ku, Kyoto 610-11

(Received 1987 August 10; accepted 1989 January 28)

Abstract

The effects of retrograde stars on the stability of flat stellar disks are examined. The models used are the isochrones with various fractions of retrograde stars. The most unstable global modes are obtained by numerically integrating the linearized collisionless Boltzmann equation. The results show that the growth rate of the one-armed mode becomes higher as the number of retrograde stars increases. On the contrary, the growth rates of the two- and three-armed modes are lowered by retrograde stars. Thus, the one-armed mode grows faster than the two- and three-armed modes when the disk contains a large number of retrograde stars. The behavior of the one-armed mode can be explained in terms of the inner Lindblad resonance of the wave with retrograde stars.

Key words: Global instabilities; Linear modal calculations; Retrograde stars; Stellar dynamics.

1. Introduction

Many N-body simulations of self-gravitating flat stellar disks have demonstrated that reasonably cool disks have a marked tendency toward bar formation [see Athanassoula (1984) for reviews and references therein]. The bar instability has also been reported in numerical simulations based on the collisionless Boltzmann equation (Nishida et al. 1984). The most popular cure for this violent instability is the addition of massive halos, which lessen the self-gravity of disks (Hohl 1971). Recent investigations have revealed that compact bulges are also effective in suppressing the bar instability (Sellwood 1985; Nishida 1986; Hozumi et al. 1987). An alternative cure, proposed by Kalnajs (1977), is to introduce retrograde stars. He indicated by means of linear theory

* Present address: Space Data Systems Engineering Department, Komukai Works, TOSHIBA Corporation, Komukai, Saiwai-ku, Kawasaki 210.

that the number of retrograde stars should lower the growth rate of bar modes.

Zang and Hohl (1978) made N-body simulations of the isochrone disk and the Schmidt–Miyamoto disk in order to verify Kalnajs's (1977) suggestion. The expected effects of retrograde stars on bar modes have been confirmed. They found, however, that a pronounced one-armed feature appears in disks with a large number of retrograde stars. Unfortunately, this peculiar behavior of one-armed modes was not studied quantitatively, because they were interested mainly in the bar modes.

At present, little is known about one-armed instabilities. This is because these are few stellar disks that are known to have unstable one-armed modes. Only two such disks exist besides the isochrone disk, to the knowledge of the present authors. One is the V=constant disk studied by Zang (1976) using linear analysis. The other is the model of our Galaxy examined by Sellwood (1985) through N-body simulations. For an understanding of one-armed modes as well as of bar modes, systematic stability analyses of a variety of models would be a desirable approach.

In this paper we examine the effects of retrograde stars on one-armed modes by using a linear stability calculation. The equilibrium model involves an isochrone disk composed of stars. This closely resembles the model studied by Zang and Hohl (1978); the only difference is that the disk is truncated at a cutoff radius in their model but not in ours. We use a numerical method based on the linearized collisionless Boltzmann equation to determine unstable modes. This method gives results which are not contaminated by the random noise which is unavoidable in N-body experiments. We can therefore obtain the growth rates and pattern speeds of normal modes with high accuracy.

The numerical method and equilibrium models are described in section 2. The results are presented in section 3. In section 4 we discuss the excitation mechanism of one-armed modes.

2. Numerical Method

The disk models examined are isochrones (Hénon 1959) which have a surface density given by

$$\Sigma(r)=(2\pi r^3)^{-1}\{\ln[r+(1+r^2)^{1/2}]-r/(1+r^2)^{1/2}\}\,, \tag{1}$$

and a potential given by

$$\Psi(r)=-[1+(1+r^2)^{1/2}]^{-1}\,, \tag{2}$$

where r is the radial distance from the center. We take the same units throughout the paper as those used by Zang and Hohl (1978).

The equilibrium distribution function is a function of the energy per unit mass, $\varepsilon=[(u^2+v^2)/2]+\Psi(r)$, and the specific angular momentum, $j=rv$, where u and v are the radial and tangential velocities, respectively. For a model composed of directly rotating stars ($j\geqq 0$), we use the equilibrium distribution function given by Kalnajs (1976):

$$F^+(\varepsilon,j)=(-\varepsilon)^{n-1}g_n(x)\,, \tag{3}$$

where x is a scaled version of $(-2\varepsilon)^{1/2}j$. The function $g_n(x)$ depends on the potential and the surface density. The integer n is related to Toomre's (1964) local stability parameter Q. Here, we take the value $n=8$. This corresponds to the typical value of Q near 1.2, ensuring the local stability of models (i.e., $Q>1$).

Retrograde stars are introduced by reversing the angular momenta of some part of directly rotating stars. This is achieved by introducing a function $b(j)$ of the form

$$b(j)=\frac{1}{2}+\frac{3}{4}\frac{j}{j_*}-\frac{1}{4}\left(\frac{j}{j_*}\right)^3 \qquad |j|\leqq j_*\,, \tag{4}$$

where $j_*=\eta j_0$. In this expression, η is a numerical factor used to specify the number of retrograde stars, and j_0 is the standard angular momentum. The value of j_0 is chosen so as to be the angular momentum of a star in circular orbit at $r=5$, as in Zang and Hohl (1978). The retrograde parameter η ($\geqq 0$) roughly determines to what extent retrograde stars are present.

With the above prescription, the equilibrium distribution functions can be written as

$$F(\varepsilon, j)=\begin{cases} F^+(\varepsilon, J) & j>j_*\,, \\ F^+(\varepsilon, |j|)b(j) & |j|\leqq j_*\,, \\ 0 & j<-j_*\,. \end{cases} \tag{5}$$

The distributions of velocities given by equation (5) are shown in figure 1 at some fixed radii for four values of η. We can see that retrograde stars extend outward as η increases, and that the distribution function in the outer region becomes two-humped when η is large.

In order to determine unstable global modes, we solve the linearized collisionless Boltzmann equation. The method used is the same as that described by Fujiwara and Hozumi (1986) and Hozumi et al. (1987). We expand the distribution function f with respect to the azimuthal angle φ around its equilibrium state F as

$$f(r, \varphi, u, j, t)=F(r, u, j)+\sum_m f_m(r, u, j, t)\exp(im\varphi)\,, \tag{6}$$

where f_m is the m-th Fourier component. The value of m (>0) corresponds to the number of spiral arms. Each Fourier component f_m in equation (6) then satisfies the linearized collisionless Boltzmann equation:

$$\frac{df_m}{dt}=\frac{\partial\psi_m}{\partial r}\frac{\partial F}{\partial u}+im\psi_m\frac{\partial F}{\partial j}\,. \tag{7}$$

The perturbed potential ψ_m is calculated from the Poisson equation:

$$\nabla^2\psi_m=4\pi\sigma_m\delta(z)\,, \tag{8}$$

where δ represents Dirac's delta function, and σ_m is the density perturbation given by

$$\sigma_m(r, t)=\frac{1}{r}\int dj\int du f_m(r, u, j, t)\,. \tag{9}$$

The fastest growing modes can be determined by solving an initial-value problem:

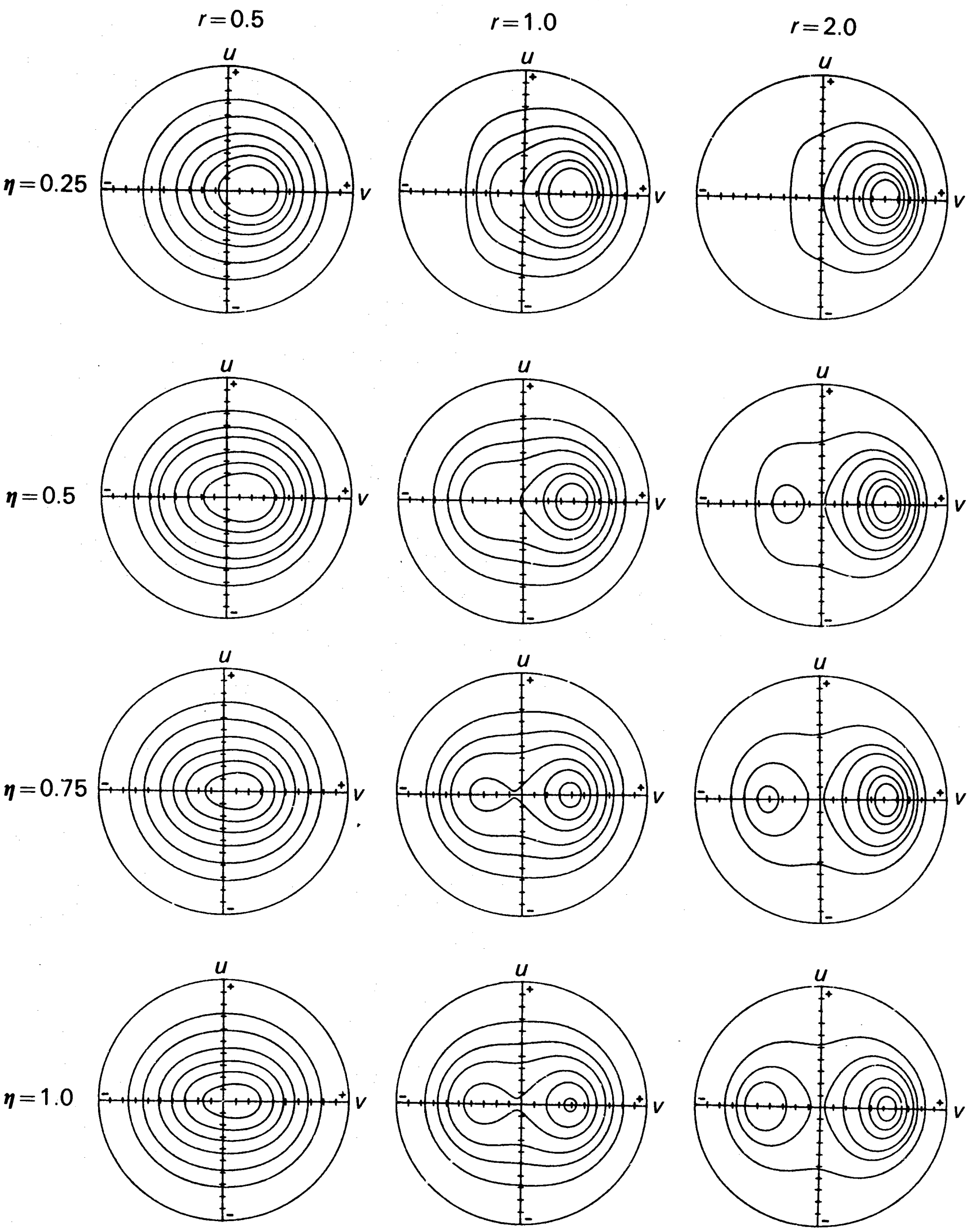

Fig. 1. Equi-frequency contours of the equilibrium distribution function for each retrograde parameters η at three different radii. The outermost circle denotes the escape velocity; u and v are the radial and tangential velocities, respectively. The contour levels are chosen arbitrary.

we impose an arbitrary initial perturbation, and integrate equation (7) numerically. Since equation (7) is linear in f_m, unstable modes, if any, grow exponentially in amplitude. Thus, we can obtain the most unstable mode if the time evolution of the perturbation is solved until it becomes purely exponential in growth. The accuracy of this method is good with a relative error of the order of 1% in both the growth rate and the pattern speed (Fujiwara and Hozumi 1986).

We set the grid points along unperturbed trajectories (i.e., along epicyclic orbits) in (ε, j)-space. The computational domain in this space is taken so that the surface density of the unperturbed disk can be reproduced up to $r \sim 10$, which is much larger than the cutoff radius $r=5$ of a truncated isochrone disk described by Zang and Hohl (1978). The second-order Runge–Kutta method is used for the time integration of equation (7). The Poisson equation (8) is solved with a biorthonormal surface density-potential set provided by Aoki and Iye (1978).

3. Results

We have examined the stability of isochrone disks with several values of η for the one-armed ($m=1$) mode. Models with $\eta=0.25$, 0.5, 0.75, and 1.0 are the same as those studied by Zang and Hohl (1978), except that the disks are not truncated. The time step used was 0.05. The results for the $m=1$ modes and the properties of the models are summarized in table 1. The growth rates and the pattern speeds of the $m=1$ modes are also plotted against η in figure 2. The growth rate rises noticeably as η increases. That is, the increase in the number of retrograde stars makes one-armed instabilities more violent. Figure 2 also shows that the $m=1$ pattern speed tends to become lower as η increases. The values of the pattern speeds are quite low, in comparison with those for the $m=2$ and $m=3$ modes (described later).

Figure 3 illustrates the density patterns of the $m=1$ modes. The dotted circle indicates the corotation radius at which the angular speed of a star, $\Omega(r)$, is equal to the pattern speed Ω_p. Because of the low pattern speed of the $m=1$ mode, the corotation circle lies well outside the central part of the disk, especially for large η. Figure 3 also shows that the pattern changes its shape from a trailing spiral type to a leading type as η increases; however, the change is small when $\eta \gtrsim 0.45$.

Figure 4 represents the orbital frequencies of stars in nearly circular orbits. For a mode rotating at a pattern speed of Ω_p, the inner Lindblad resonance occurs in the region where the condition $\Omega(r)-[\kappa(r)/m]=\Omega_p$ is satisfied (κ is the epicyclic frequency). As shown in figure 4, $\Omega-(\kappa/m)$ is negative for $m=1$. Since the $m=1$ modes rotate in the positive direction (i.e., $\Omega_p>0$), it can be seen that they have no inner Lindblad resonance.

For the sake of comparison, we have performed stability calculations for two- and three-armed modes. The equilibrium models are the same as those for the $m=1$ mode.

Table 1. Summary of the models and the results for $m=1$ modes.

η	Growth rate	Pattern speed	Random energy in tangential motion	Fraction of retrograde stars (%)
0.25........	0.0247	0.114	0.00519	4.72
0.30........	0.0423	0.122	0.00592	5.42
0.35........	0.0614	0.115	0.00668	6.10
0.40........	0.0734	0.104	0.00747	6.76
0.45........	0.0815	0.0937	0.00828	7.40
0.50........	0.0878	0.0847	0.00910	8.02
0.75........	0.102	0.0573	0.0133	10.9
1.00........	0.107	0.0432	0.0173	13.5

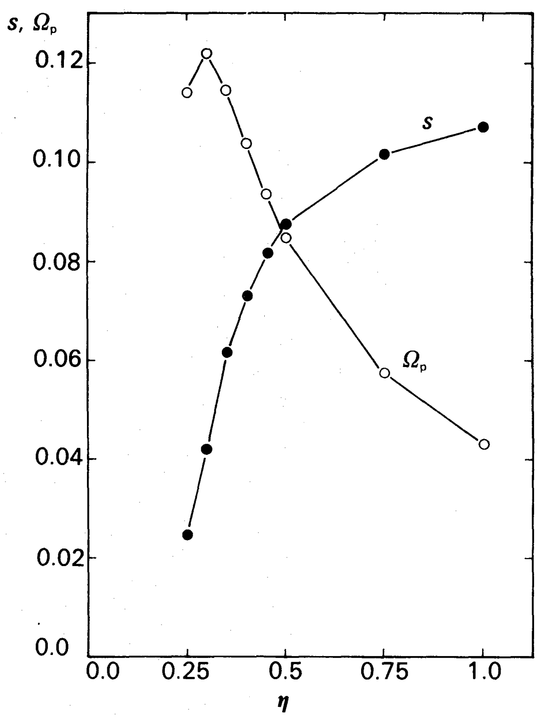

Fig. 2. The growth rate s (closed circle) and the pattern speed Ω_p (open circle) of the $m=1$ mode plotted against η.

We take $\eta=0.25$, 0.5, 0.75, and 1.0. Figure 5 presents the growth rates and the pattern speeds for $m=2$ and $m=3$. In contrast to the results for the $m=1$ modes, an increase in the number of retrograde stars certainly lowers the growth rates of the $m=2$ and $m=3$ modes. The pattern speeds decrease with η for both the $m=2$ and $m=3$ modes. In the isochrone disk, the maximum value of $\Omega(r)-[\kappa(r)/m]$ is 0.059 for $m=2$, and 0.167 for $m=3$ (cf. figure 4). It can be seen from figure 5 that the pattern speeds of the $m=2$ and $m=3$ modes are higher than the above-mentioned values, respectively; therefore, no inner Lindblad resonance occurs. The winding sense of all $m=2$ and $m=3$ modes was trailing.

The results presented here show that the destabilizing effect of retrograde stars is peculiar only to the $m=1$ mode. It can also be seen that for models with $\eta \geqq 0.5$, the $m=1$ mode grows faster than the $m=2$ and $m=3$ modes. This explains the noticeable one-armed features which appeared in the models with large η in the N-body simulations by Zang and Hohl (1978).

4. Discussion

We have shown that the growth rate of the $m=1$ mode increases with the number of retrograde stars. We now discuss whether this behavior of the $m=1$ mode can be explained in terms of existing local theories of density waves.

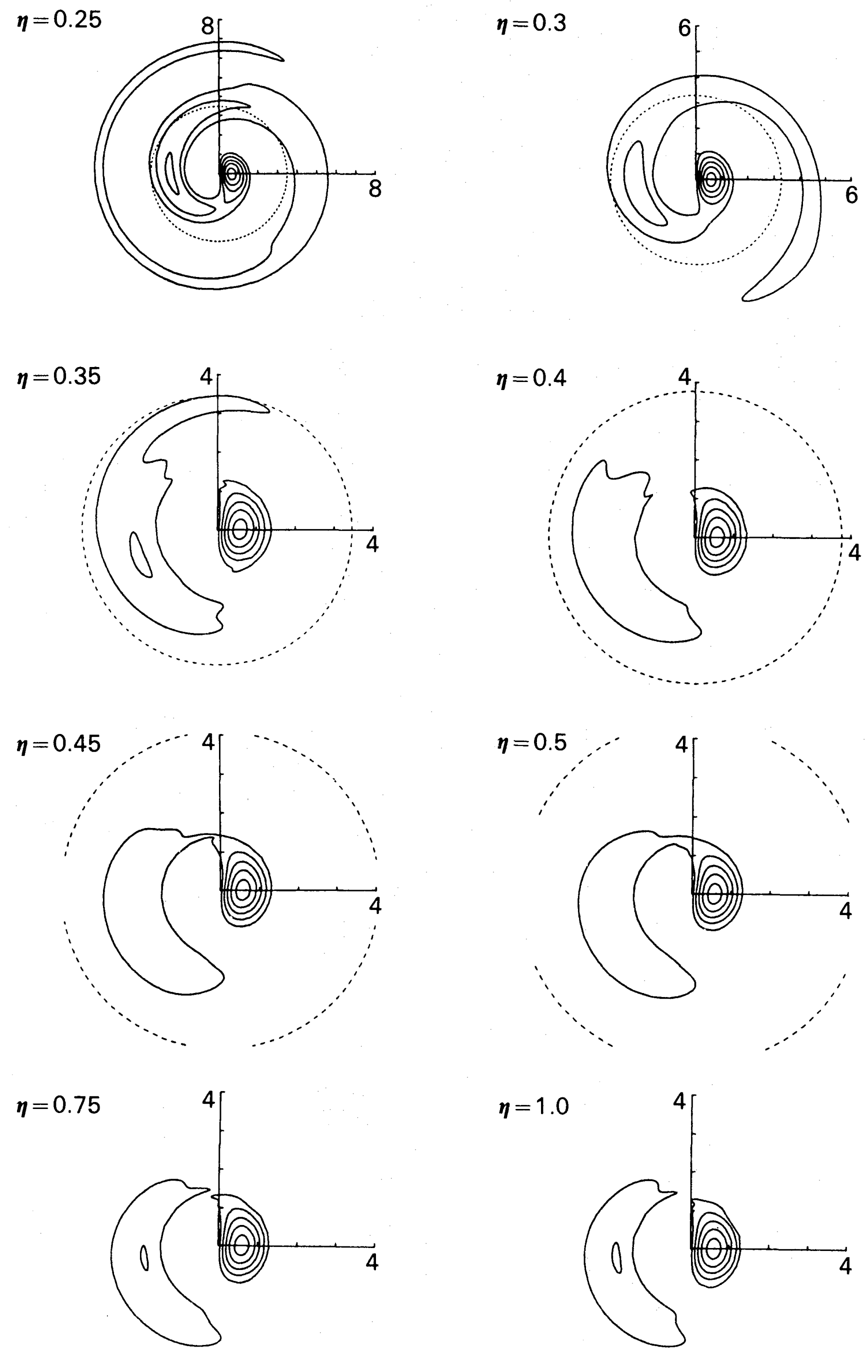

Fig. 3. Density distributions of the $m=1$ modes. The density contours are drawn at the 10, 30, 50, 70, and 90% levels of the peak amplitude. Dotted circles indicate the corotation radii. The rotation is counterclockwise.

(1) Wave Amplification near the Corotation Circle

Such an amplification of density waves as WASER (Mark 1976) or swing amplification (Toomre 1981) are widely accepted as an exciting mechanism of unstable global modes. To complete the feedback cycle, WASER requires the reflection of inward traveling waves near the center, while swing amplification requires a passable center.

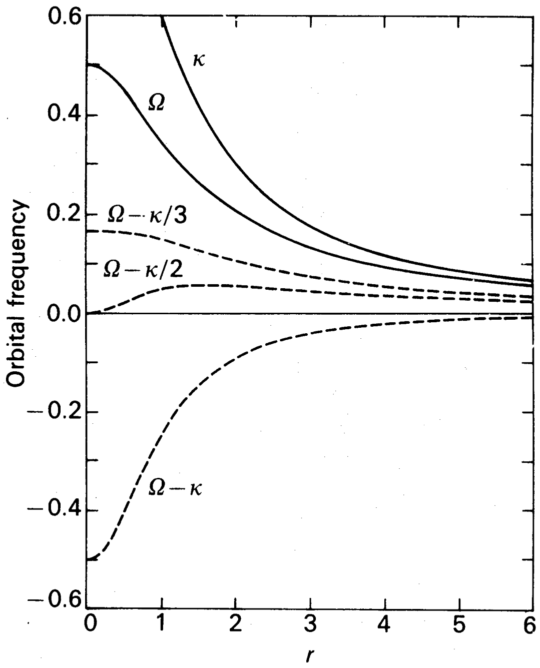

Fig. 4. The rotation frequency Ω, the epicyclic frequency κ, and their combinations, for the isochrone disk.

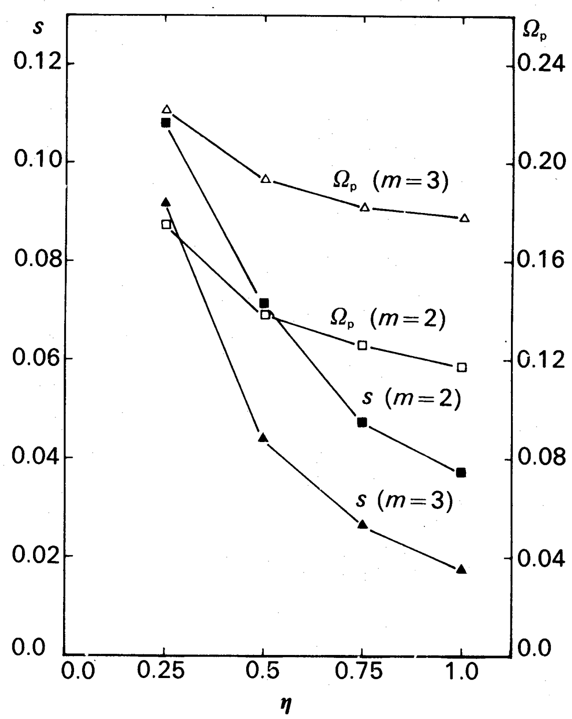

Fig. 5. The growth rates s (closed symbols) and the pattern speeds Ω_p (open symbols) of the $m=2$ (squares) and $m=3$ (triangles) modes plotted against η.

In our models WASER does not work because the Q-value of the central part is not sufficiently high to reflect waves. On the other hand, the absence of the inner Lindblad resonance which absorbs the wave satisfies the requirement for swing amplification.

The swing-amplification explanation encounters a difficulty in accounting for the tendency of the $m=1$ growth rate. In an interpretation of swing amplification, the growth rate is determined by two factors: the amplification factor of the wave when it swings near the corotation circle, and the time required for the wave to complete the cycle. The slow pattern speed of the $m=1$ mode means that the corotation circle lies in a region of low surface density; this makes the amplification factor quite small. The large corotation radius also leads to a long travel time of the wave. Thus, swing amplification predicts low growth rates for slowly rotating modes. This is contrary to the $m=1$ results. We may conclude that the $m=1$ mode is not a swing-amplified one. It should be noted that the behavior of the $m=2$ and the $m=3$ modes is reasonably explained by swing amplification.

(2) Landau Growing Mode

Marochnik and Suchkov (1969) and Takahara et al. (1976) studied the stability of disk-halo systems by using the WKBJ approximation, and found that the Landau growing mode due to the resonant interaction of the density wave with halo stars exists in such systems. Since the distribution functions of our models have a two-humped feature, like those of disk-halo systems, the Landau instability is expected in our models as well. Here we examine the possibility that the $m=1$ modes are Landau growing modes.

The spiral pattern of the $m=1$ mode shown in figure 3 is close to a sector, especially for large η. It would therefore be reasonable to regard the $m=1$ pattern as a wave running in the tangential direction. If we consider such a wave for simplicity, then a resonant interaction occurs for stars with a tangential velocity v equal to the phase velocity of the wave, $v_{\mathrm{ph}}=r\Omega_{\mathrm{p}}$. Since the energy of the wave is negative within the corotation circle, the condition for the Landau instability can be written as

$$dF_1/dv\big|_{v=v_{\mathrm{ph}}}<0\,, \tag{10}$$

where $F_1(v)=\int F(u, v)du$. If this condition is satisfied over a wide range of the disk, unstable global modes might appear. However, the derivative in equation (10) is positive at any radius within the corotation circle (see figure 1). Thus, the growing condition is not satisfied. The situation is almost the same even if we choose the wave running in other directions. It is difficult to regard the $m=1$ mode as a Landau growing type.

(3) Inner Lindblad Resonance with Retrograde Stars

For $m=1$, the inner Lindblad resonance (ILR) does not occur for a wave with $\Omega_{\mathrm{p}}>0$. This statement is true as long as resonance with directly rotating stars is involved. In a disk containing retrograde stars, however, the ILR of the $m=1$ wave with retrograde stars is possible because the angular speed and the epicyclic frequency of these stars are negative. That is, the condition for this kind of ILR can be written as $-(\Omega-\kappa)=\Omega_{\mathrm{p}}$, where Ω and κ are positive (i.e., those for directly rotating stars); this can be satisfied for a wave with $\Omega_{\mathrm{p}}>0$, as shown in figure 4. As is known, the usual ILR (e.g., that of the $m=2$ wave with directly rotating stars) absorbs the wave. We now consider the role of the ILR with retrograde stars.

The exchange of the angular momentum and the energy between resonant stars and the wave has been investigated in detail by Kalnajs (1971) and by Lynden-Bell and Kalnajs (1972). Since the present models are dominated by directly rotating stars, the wave has negative angular momentum and negative energy within the corotation circle, as in usual disks. Therefore, the wave will be dampened if stars feed it with energy, but will grow if stars absorb energy from it.

According to equation (29) of Lynden-Bell and Kalnajs (1972), resonant retrograde stars in the region of the ILR lose their absolute angular momentum as a whole. This means that the change in the angular momentum of resonant stars, δj, is positive. The corresponding change in the energy of resonant stars, $\delta\varepsilon$, is then positive because $\delta\varepsilon$ is related to δj as $\delta\varepsilon=\Omega_{\rm p}\delta j$ [see section 5 of Lynden-Bell and Kalnajs (1972)]. That is, resonant stars absorb energy from the wave. Thus, we see that retrograde stars in the region of the ILR can excite the wave.

The results for the $m=1$ modes can be explained in terms of the ILR with retrograde stars. As η increases, retrograde stars extend outward, in such a way that the resonance in the outer region becomes more important. This accounts for the decrease in the pattern speed of the $m=1$ mode with η (cf. figure 4). The increase in the number of retrograde stars also causes the excitation of the wave to be more efficient. This gives a natural explanation for the increase in the $m=1$ growth rate with η.

From figure 3, it can be seen that the secondary peak of the density perturbation appears at $r\sim 2$. This location is close to the radius of the ILR with retrograde stars, $r\sim 2$–3 (cf. figure 4). This also suggests that the $m=1$ modes are excited in the region of the ILR. For modes with small η ($\lesssim 0.3$), swing amplification as well as the ILR probably plays an important role in wave excitation, since the peak appears just inside the corotation circle for such modes. The density peak near the center may be the interference pattern of an inward-running wave with one which has passed through the center.

If the excitation mechanism of the $m=1$ mode is the ILR with retrograde stars, the energy taken from the wave will be liberated into the noncircular motion of resonant stars. Such an evolution of the disk should be observed if we make a numerical experiment in the nonlinear regime. The picture of the ILR with retrograde stars also suggests that the efficiency of the wave excitation is closely related to the form of the distribution function: if the velocity dispersion of retrograde stars is so large that the epicyclic approximation fails, then the wave excitation by the ILR will be of little importance.

Since the present investigation is concerned only with the isochrone disk, it remains unclear whether one-armed modes of a wide variety of disks can be understood by the picture given above. We should examine such models, for example, as "hot" disks or those that have retrograde stars introduced in a different manner. Recently, Sawamura (1988) found that similar one-armed instabilities exist in a series of stellar disks of finite radius.

We would like to thank Professor S. Kato for his encouragement, and Drs. S. Inagaki, M. T. Nishida, and Professor P. Hut for their helpful discussions. We are also grateful to Dr. M. Yoshizawa, the referee, for useful comments for improving the paper. This work was supported by a Grant-in-Aid for Scientific Research of the Ministry of Education, Science, and Culture (60540159). Numerical computations were carried out at the Data Processing Center of Kyoto University.

References

Aoki, S., and Iye, M. 1978, *Publ. Astron. Soc. Japan*, **30**, 519.
Athanassoula, E. 1984, *Phys. Rept.*, **114**, 319.
Fujiwara, T., and Hozumi, S. 1986, *Astrophys. Space Sci.*, **119**, 199.
Hénon, M. 1959, *Ann. Astrophys.*, **22**, 126.
Hohl, F. 1971, *Astrophys. J.*, **168**, 343.
Hozumi, S., Fujiwara, T., and Nishida, M. T. 1987, *Publ. Astron. Soc. Japan*, **39**, 447.
Kalnajs, A. J. 1971, *Astrophys. J.*, **166**, 275.
Kalnajs, A. J. 1976, *Astrophys. J.*, **205**, 751.
Kalnajs, A. J. 1977, *Astrophys. J.*, **212**, 637.
Lynden-Bell, D., and Kalnajs, A. J. 1972, *Monthly Notices Roy. Astron. Soc.*, **157**, 1.
Mark, J. W.-K. 1976, *Astrophys. J.*, **205**, 363.
Marochnik, L. S., and Suchkov, A. A. 1969, *Astrophys. Space Sci.*, **4**, 317.
Nishida, M. T. 1986, *Astrophys. J.*, **302**, 611.
Nishida, M. T., Watanabe, Y., Fujiwara, T., and Kato, S. 1984, *Publ. Astron. Soc. Japan*, **36**, 27.
Sawamura, M. 1988, *Publ. Astron. Soc. Japan*, **40**, 279.
Sellwood, J. A. 1985, *Monthly Notices Roy. Astron. Soc.*, **217**, 127.
Takahara, F., Ikeuchi, S., and Nakamura, T. 1976, *Prog. Theor. Phys.*, **55**, 1743.
Toomre, A. 1964, *Astrophys. J.*, **139**, 1217.
Toomre, A. 1981, in *The Structure and Evolution of Normal Galaxies*, ed. S. M. Fall and D. Lynden-Bell (Cambridge University Press, Cambridge), p. 111.
Zang, T. A. 1976, Ph. D. Thesis, Massachusetts Institute of Technology.
Zang, T. A., and Hohl, F. 1978, *Astrophys. J.*, **226**, 521.